Accuracy and uncertainty of single-shot, nonresonant laser-induced thermal acoustics

Stefan Schlamp, Hans G. Hornung, Thomas H. Sobota, and Eric B. Cummings

We study the accuracy and uncertainty of single-shot nonresonant laser-induced thermal acoustics measurements of the speed of sound and the thermal diffusivity in unseeded atmospheric air from electrostrictive gratings as a function of the laser power settings. For low pump energies, the measured speed of sound is too low, which is due to the influence of noise on the numerical data analysis scheme. For pump energies comparable to and higher than the breakdown energy of the gas, the measured speed of sound is too high. This is an effect of leaving the acoustic limit, and instead creating finite-amplitude density perturbations. The measured thermal diffusivity is too large for high noise levels but it decreases below the predicted value for high pump energies. The pump energy where the error is minimal coincides for the speed of sound and for the thermal diffusivity measurements. The errors at this minimum are 0.03% and 1%, respectively. The uncertainties for the speed of sound and the thermal diffusivity decrease monotonically with signal intensity to 0.25% and 5%, respectively.

OCIS codes: 000.2170, 050.2770, 120.6780, 190.4380.

1. Introduction

In the four-wave mixing technique of laser-induced thermal acoustics (LITA), two pulsed laser beams (excitation beams) intersect at a shallow angle in the test gas where interference creates an electric field grating. By the molecular mechanisms of electrostriction and thermalization, the electric field grating results in a density perturbation and hence a refractive-index grating. Thermalization is predominant for resonant pumping, whereas electrostrictive gratings dominate in the case of nonresonant pumping. If a continuous laser beam is directed at the Bragg angle at the density grating, part [$\mathcal{O}(0.01\%)$] of this interrogation beam is coherently scattered into a signal beam. Because the density grating evolves over time and the signal beam intensity is proportional to the instantaneous density grating modulation depth, the signal beam allows us to observe the grating evolution.

The speed of sound is encoded in the LITA signal as the Brillouin frequency, i.e., the speed of sound divided by the fringe spacing of the density grating. The thermal diffusivity together with the Gaussian beam profiles cause the exponentially decaying tail of a LITA signal (Fig. 1). To extract the speed of sound and the thermal diffusivity from a LITA signal we used a theoretical model[1,2] and a nonlinear fitting procedure (Levenberg–Marquardt scheme[3]) that fit this model to the experimental data. The speed of sound and the thermal diffusivity are fitting parameters. The fringe spacing and the beam sizes are determined in a calibration measurement at known fluid conditions. A frequency decomposition technique to extract the Brillouin frequency from the signal is also possible[4] but it does not allow for measurements of the thermal diffusivity. The same is true when the Prony method is used to extract the speed of sound.[5,6]

The accuracy (i.e., the systematic error) and the uncertainty (i.e., the statistical error) of this method depend on a number of parameters. The accuracy of the calibration measurement, i.e., knowledge of the precise fringe spacing and the Gaussian beam halfwidths, limits the measurement accuracy. The uncertainty of the Brillouin frequency will be reduced if many oscillation cycles are recorded in the signal and

S. Schlamp (stefan@galcit.caltech.edu) and H. G. Hornung (hans@galcit.caltech.edu) are with the Aeronautical Laboratory, California Institute of Technology, Pasadena, California 91125. T. H. Sobota (thsobota@advancedprojects.com) is with Advanced Projects Research, Incorporated, 1925 McKinley Avenue, La Verne, California 91750. E. B. Cummings (labsmith@home.com) is with Sandia National Laboratories, Livermore, California 94551.

Received 14 February 2000; revised manuscript received 22 June 2000.

0003-6935/00/305477-05$15.00/0

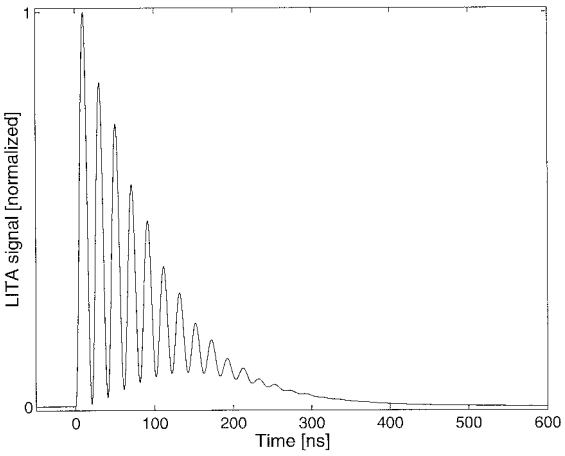

Fig. 1. LITA signal from electrostrictive gratings in atmospheric air (32-shot average).

if the time resolution is good. Similarly, we want the total signal recording time and sampling rate to be appropriate for the decay time constant of the signal tail. In addition, the accuracy and uncertainty of LITA measurements are mostly limited by two factors: noise in the recorded signals and deviations of the theoretical model from experiment. These latter two factors are examined here.

To raise the signal-to-noise ratio (SNR) at a fixed noise level one can increase either the excitation laser-pulse energy or the interrogation beam power (or both). Theoretically, the signal should be proportional to the interrogation laser power and should scale quadratically with the excitation laser-pulse energy,[7] provided that all other experimental parameters are held constant (beam crossing angle, beam geometry, detector sensitivity, etc.).

The theory used in the fitting assumes that the density perturbations caused by the excitation laser are small compared with the ambient density, i.e., that the density grating behaves like an acoustic wave. This approximation becomes worse with increasing excitation laser-pulse energies. We see that there will be a trade-off between the favorable influence of a stronger signal and the negative effects of the nonlinear behavior of the waves. We want to study this trade-off and find the point of best accuracy and lowest uncertainty.

2. Experimental Setup and Procedure

A frequency-doubled, *Q*-switched Nd:YAG laser (Continuum Surelite I10, maximum of 250 mJ, 10 Hz) was used as the excitation laser. An arrangement of beam splitters and mirrors on kinematic mounts splits the beam in halves and focuses them pathlength matched on a finite-size point (the sample volume) where they intersect at an angle of 2.175°. The Gaussian beam half-width in the sample volume is 180 μm as determined in a calibration measurement. The sample volume was located in the (air-conditioned) ambient room air without a surrounding test cell. We adjusted the pulse energy by varying the flash-lamp voltage. The excitation laser-pulse energy at different flash-lamp voltages was measured with a laser powermeter (Scientech Astral AA30). Pulse energies ranged from 17 to 110 mJ. The data acquisition was triggered by a photodetector (Thorlabs DET210, 1-ns response time) that detected the excitation laser pulse.

A cw argon-ion laser (Spectra-Physics Stabilite 2017, maximum of 1.3 W at 488 nm) provides the interrogation beam. The signal beam that is coherently scattered off the density grating is detected by a photomultiplier tube (Hamamatsu H5783-03, 0.65-ns response time) and recorded as 2048 discrete points with 12-bit resolution on a digital storage oscilloscope (Hewlett-Packard Infinium, 500 MHz) from where it transferred to a personal computer for storage and data analysis. We removed incoherently scattered light from the signal beam by employing an interference filter and a spatial filter. Figure 1 shows that the signals have no contributions stemming from the excitation beam which would show as a short peak at $t = 0 \ldots 8$ ns. We aligned the optics by imaging onto a screen the sample volume using a lens. This allowed us to inspect the interference fringes visually and the position of the interrogation beam relative to the sample volume.

Sets of 1000 single-shot measurements were recorded for a range of excitation laser pump energies. These sets were taken in random order to eliminate systematic errors, e.g., errors that are due to variations in air temperature. The continuous interrogation beam was operated at full power for most measurements. Only when the lower limit for the flash-lamp voltage (preset by the manufacturer) was reached, the interrogation laser power was reduced to decrease the signal level further. A pulse energy that resulted in gas breakdowns in more than 10% of the shots was taken as the upper limit. Shots in which a gas breakdown occurred were discarded from the subsequent data analysis.

The system was calibrated with twenty 32-shot-averaged signals obtained at intermediate power settings (Fig. 1). Ten calibration signals were taken at the beginning of the tests, and ten were taken at the end. No significant difference was observed between the two groups of signals. A speed of sound of 345 m/s was assumed for these calibration signals. Lacking precision temperature, pressure, and humidity data, we could not determine the exact speed of sound. But because the measured speed of sound is proportional to the assumed speed of sound in the calibration, errors made in this assumed speed of sound cancel with resulting errors in the actual data. This means that, although the measured speed of sound depends on an accurate calibration, the resulting values for the accuracy and uncertainty do not. The calibration resulted in a beam crossing angle of $\theta = 2.175°$, an excitation beam half-width of $\omega = 189$ μm, and an interrogation beam half-width of $\sigma = 330$ μm. The beam geometries were assumed independent of the laser power settings. We determined the sound speed and the thermal diffusivity for every

trace using a Levenberg–Marquardt fitting[3] of a theoretical model to the experimental data.[1,2] The deviation of the average sound speed (thermal diffusivity) over a set from the calibration value

$$\Delta c_s = \frac{c_{s,meas} - c_{s,calib}}{c_{s,calib}}, \quad \Delta D_T = \frac{D_{T,meas} - D_{T,calib}}{D_{T,calib}}$$

was used as the systematic error caused by laser intensity changes. The standard deviation of the sound speed (thermal diffusivity) over each set was taken as the measure for the uncertainty (statistical error).

3. Results

Figure 2 shows the SNR versus the square of the driver-laser-pulse energy (E_d) times the interrogation beam power (P_0). We define the SNR as the peak signal intensity of a given signal divided by the standard deviation of the noise in the pretrigger part of the signal. As the theory predicts,[7] the signal intensity is approximately proportional to the interrogation beam power and scales with the square of the driver-laser-pulse energy. For high driver beam energies, the signals are stronger than predicted. The calibration measurement stands out because we obtained it by averaging over 32 individual traces, resulting in an approximately six times higher SNR at a given driver-laser-pulse energy. Deviations from the dashed line are most likely due to errors in the measurement of P_0 and E_d.

Figure 3 illustrates how, at high pump energies, a gas breakdown can occur in the sample volume. It plots the likelihood of observed gas breakdowns versus the driver laser energy in the sample volume. Below a critical pump energy no gas breakdowns are observed but their likelihood increases linearly for pump energies above that threshold. The relevant physical quantity for the gas breakdown is the electric field grating intensity. Hence the threshold value for the driver laser pump energy will be a function of the pulse duration, beam diameter and quality, beam crossing angle, and also of the test gas. Particulates in the test gas critically influence the breakdown energy. For the test gas used, the critical pump energy is 50 mJ, which, according to Fig. 2 (P_0 = 1.3 W), corresponds to a SNR of 80.

The error and uncertainty of the sound speed measurements are plotted in Fig. 4. Similarly, Fig. 5 shows these results for the thermal diffusivity measurements. For low SNR's, the measured speed of sound is too low. The error passes through zero at a SNR of 110 (minimum error is 0.03%). For higher pump energies, the measured speed of sound is too high. The uncertainty does not have a minimum but instead decreases monotonically with increasing signal level. The error in the calibration signals is zero by construction.

The uncertainty for the thermal diffusivity measurements also decreases monotonically with increasing signal intensity. It is, however, approximately ten times higher than for the sound speed

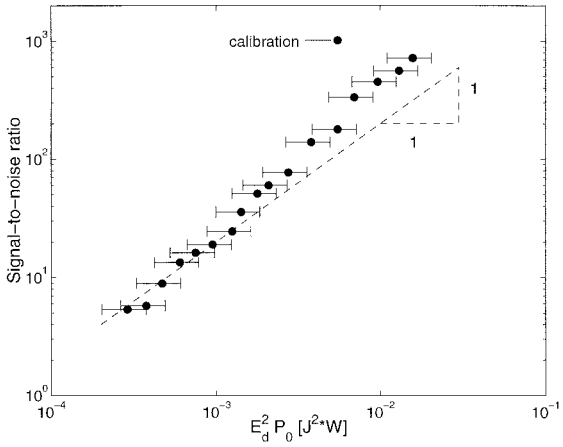

Fig. 2. SNR versus $E_d^2 P_0$ where E_d is the driver-laser-pulse energy and P_0 is the interrogation beam power.

measurements at the same signal intensity. The trend for the accuracy for the thermal diffusivity is less pronounced but it appears to show the same behavior as the sound speed error with a minimum that coincides with the minimum for the sound speed measurements (the SNR is approximately 100). The measured thermal diffusivity tends to be too high for SNR's above the optimum and drops below the calibration value for SNR's greater than 100.

4. Discussion and Conclusions

The initial drop in the error and uncertainty with increasing laser power settings can be attributed to the increase in the SNR. The sign of the error will depend on the numerical scheme used for the data analysis. The Levenberg–Marquardt scheme seemingly tends to smear out the oscillations in the presence of noise, resulting in a speed of sound that is too low. The increased error for high SNR's is due to high-excitation beam pulse energies. The density waves for these conditions can no longer be considered to be infinitesimally weak, which violates a basic

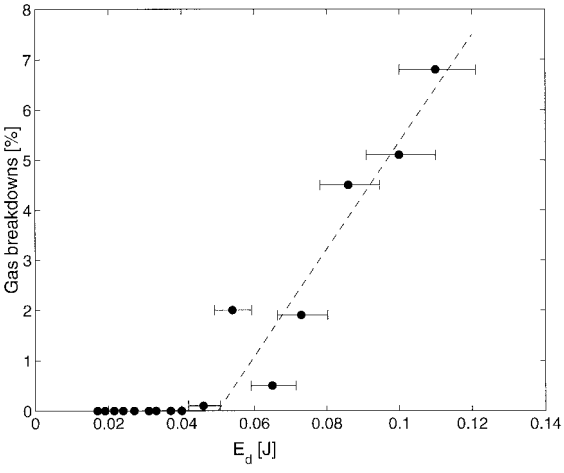

Fig. 3. Percentage of shots with gas breakdown in the sample volume versus the driver-laser-pulse energy density.

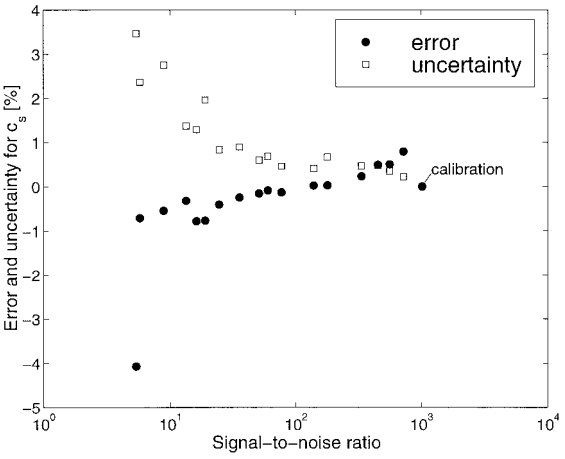

Fig. 4. Error and uncertainty of the speed of sound versus the SNR.

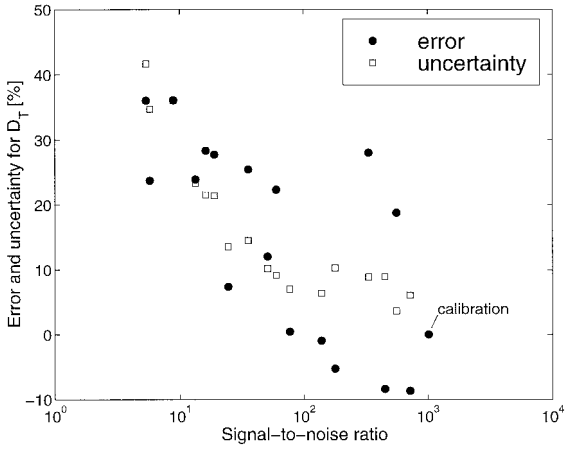

Fig. 5. Error and uncertainty for the thermal diffusivity versus the SNR.

assumption in the theoretical model that is used in the fitting routine. Instead, finite-amplitude disturbances with changing wave shapes are created that travel faster than the local speed of sound of the undisturbed fluid,[8,9] resulting in measured speeds of sound that are above the correct value. This also causes the density perturbations (and hence the signal intensity) to be stronger than for acoustic waves (Fig. 2). Another possible explanation of the higher measured speed of sound at high pump energies is local heating. But the lack of features in the signals from the signals that we obtained by measurements with thermalization gratings[1,2] indicates that local heating is not significant.

The sign of the error in the measurements of the thermal diffusivity could also depend on the numerical scheme used. In the present case, the effect of noise is that the fitting routine underpredicts the decay time constant, i.e, overpredicts the thermal diffusivity. The measured thermal diffusivity depends on the beam sizes that were determined in the calibration at a given power setting. Variations of the beam geometry as a function of the excitation laser power setting can also lead to this result. Future measurements will compare the results when the pulse energy is controlled by either the flash-lamp voltage or by means of the Q-switch delay.

The optimum pulse energy in our case is slightly above the critical value that can cause gas breakdowns. At this point we should have already left the acoustic limit, but the benefits of the high SNR still prevail. At this point, the tendency of the numerical scheme to smear out oscillations is offset by the nonlinear acoustic effects. This optimum point will depend on the experimental setup that is used. The errors for single-shot measurements that are due to laser intensity changes at the optimum pump energy are 0.03% and 1% for the speed of sound and the thermal diffusivity, respectively. The uncertainties at this point of best accuracy are 0.5% and 10%, respectively.

Averaging over many driver laser shots offers the possibility of remaining in the acoustic limit while at the same time increasing the SNR (Fig. 2). Similarly, high interrogation beam powers with lower driver-laser-pulse energies have to be preferred over the opposite case, e.g. by use of long-pulsed, high-intensity interrogation beams.[10] Also, photomultipliers with high quantum efficiencies will result in an increased signal level at a given driver-laser-pulse energy. These measures will move the point of minimal error toward lower driver laser energies. The gas breakdown energy is sensitive with respect to the type and concentration of particulates in the test gas. In a particle-free gas with otherwise unchanged conditions, the optimal pump energy does remain constant but gas breakdowns will be observed only for pump energies higher than those listed in Fig. 3.

The reason for the higher errors for the measurement of the thermal diffusivity is twofold. First, given a sufficient time resolution and number of cycles in the signal, we can measure a frequency much more precisely than a decay time constant. This is particularly true in the presence of noise. Second, to convert the measured Brillouin frequency into the speed of sound, only two parameters play a role: the driver beam wavelength and the driver beam crossing angle. The wavelength is fixed, constant, and precisely known. The bandwidth of the laser is negligible. The beam crossing angle is stable. Depending on the optical setup, pointing instabilities of the driver laser will not change it. We can determine it in a calibration measurement within $\pm 0.01\%$.[7] The conversion of the decay time constant into the thermal diffusivity requires knowledge of the driver beam half-width and the interrogation beam half-width in the sample volume. Furthermore, the theory assumes Gaussian beam profiles, and deviations therefrom will lead to errors. Each of these parameters carries an uncertainty, and the beam geometries especially will vary because of thermal effects in the lasers.

The uncertainties are not influenced by the deviation of the theory from experiment as this represents a systematic rather than a statistical error. Hence they decrease monotonically with increasing driver-laser-pulse energy (SNR). The results should also apply in similar fashion to LITA when resonant pumping is used and to other techniques for signal processing.[4,5]

This research was supported by Advanced Projects Research, Inc. and by NASA Langley Research Center under NASA contract NAS1-99016.

References

1. E. B. Cummings, I. A. Leyva, and H. G. Hornung, "Laser-induced thermal acoustics (LITA) signals from finite beams," Appl. Opt. **34,** 3290–3302 (1995).
2. S. Schlamp, E. B. Cummings, and H. G. Hornung, "beam misalignments and fluid velocities in laser-induced thermal acoustics (LITA)," Appl. Opt. **38,** 5724–5733 (1999).
3. W. H. Press, *Numerical Recipes in C*: *the Art of Scientific Computing* (Cambridge U. Press, New York, 1988).
4. A. Stampanoni-Panariello, B. Hemmerling, and W. Hubschmid, "Temperature measurements in gases using laser-induced electrostrictive gratings," Appl. Phys. B **67**(1), 125–130 (1998).
5. R. C. Hart, R. J. Balla, and G. C. Herring, "Non resonant referenced laser-induced thermal acoustics thermometry in air," Appl. Opt. **38,** 577–584 (1999).
6. S. L. Marple, *Digital Spectral Analysis with Applications* (Prentice-Hall, Englewood Cliffs, N.J., 1987).
7. E. B. Cummings, "Laser-induced thermal acoustics," Ph.D. dissertation (California Institute of Technology, Pasadena, Calif., 1995).
8. A. H. Shapiro, *The Dynamics and Thermodynamics of Compressible Fluid Flow* (Wiley, New York, 1953), Vol. 2.
9. H. W. Liepmann and A. Roshko, *Elements of Gasdynamics* (Wiley, New York, 1957).
10. D. J. W. Walker, R. B. Williams, and P. Ewart, "Thermal grating velocimetry," Opt. Lett. **23,** 1316–1318 (1998).